SCIENCE CHINA Materials ARTICLES

mater.scichina.com link.springer.com

Published online 6 June 2019 | https://doi.org/10.1007/s40843-019-9444-y
Sci China Mater 2019, 62(10): 1479–1487

Membraneless reproducible MoS_2 field-effect transistor biosensor for high sensitive and selective detection of FGF21

Xinxing Gong[1†], Yeru Liu[1†], Haiyan Xiang[1], Hang Liu[1], Zhigang Liu[2], Xiaorui Zhao[1], Jishan Li[1], Huimin Li[1], Guo Hong[3], Travis Shihao Hu[4], Hong Chen[5], Song Liu[1*] and Gang Yu[1*]

ABSTRACT Fibroblast growth factor 21 (FGF21) serves as an essential biomarker for early detection and diagnosis of non-alcoholic fatty liver disease (NAFLD). It has received a great deal of attention recently in efforts to develop an accurate and effective method for detecting low levels of FGF21 in complex biological settings. Herein, we demonstrate a label-free, simple and high-sensitive field-effect transistor (FET) biosensor for FGF21 detection in a nonaqueous environment, directly utilizing two-dimensional molybdenum disulfide (MoS_2) without additional absorption layers. By immobilizing anti-FGF21 on MoS_2 surface, this biosensor can achieve the detection of trace FGF21 at less than 10 fg mL^{-1}. High consistency and satisfactory reproducibility were demonstrated through multiple sets of parallel experiments for the MoS_2 FETs. Furthermore, the biosensor has great sensitivity to detect the target FGF21 in complex serum samples, which demonstrates its great potential application in disease diagnosis of NAFLD. Overall, this study shows that thin-layered transition-metal dichalcogenides (TMDs) can be used as a potential alternative platform for developing novel electrical biosensors with high sensitivity and selectivity.

Keywords: FGF21, MoS_2, FET biosensor, disease diagnostics

INTRODUCTION

With the rapid lifestyle, diet and habit changes, non-alcoholic fatty liver disease (NAFLD) has becoming a significant risk factor as one of the major chronic liver diseases in developed countries such as Europe, the United States and in rich areas of China [1]. The NAFLD occurrence in general adults is 10% to 30%, and it has become a major cause of liver diseases which can progress to non-alcoholic steatohepatitis (NASH), cirrhosis, and hepatocellular carcinoma (HCC) [2,3]. The detection of biomarkers at the earliest stage is of great significance to NAFLD diagnostics. A new metabolic regulator, fibroblast growth factor 21 (FGF21), has decisive effects on lowering blood glucose, lipids and insulin levels, reversing hepatic steatosis, and increasing insulin sensitivity [4,5]. Previous studies have shown that FGF21 plays a crucial role in liver metabolism and serves as a potential NAFLD marker. The level of FGF21 in blood plasma is an important indicator for patients with NAFLD [6]. At this stage, the method for detecting FGF21 by enzyme-linked immunosorbent assay (ELISA) is highly selective and commonly practiced; however, this method has some critical disadvantages such as complicated sample processing, high cost, limited applications in real-time monitoring, and low detection sensitivity [7,8]. Hence, developing robust assay platforms to enable an accurate and efficient detection of low-level FGF21 in complex biological samples is still a challenging topic.

In recent years, field-effect transistors (FETs) have been proposed as one of the most promising electrical technologies for rapid biomolecule detection due to their label-free, *in-situ* detection capabilities, and high sensitivity

[1] Institute of Chemical Biology and Nanomedicine (ICBN), State Key Laboratory of Chemo/Biosensing and Chemometrics, College of Chemistry and Chemical Engineering, Hunan University, Changsha 410082, China
[2] Department of Head and Neck Oncology, The Cancer Center of the Fifth Affiliated Hospital of Sun Yat-sen University, Phase I Clinical Trial Laboratory, The Fifth Affiliated Hospital, Sun Yat-sen University, Zhuhai 519001, China
[3] Institute of Applied Physics and Materials Engineering, University of Macau, Avenida da Universidade, Taipa, Macau, China
[4] Department of Mechanical Engineering, California State University, Los Angeles, CA 90032, USA
[5] School of Materials Science and Energy Engineering, Foshan University, Foshan 528000, China
[†] These authors contributed equally to this work.
[*] Corresponding authors (emails: liusong@hnu.edu.cn (Liu S); yuganghnu@163.com (Yu G))

[9,10]. One-dimensional (1D) semiconductors, such as silicon nanowires (SiNWs) [11,12] and carbon nanotubes (CNTs) are used for FET biosensors, which can improve the sensitivity due to high switching characteristics (high current switching ratio) and excellent surface chemistry efficiency [13,14]; however, there are some limitations such as the lack of practical applications due to device-to-device deviation and relatively high cost in large-scale manufacturing [10]. Compared to 1D nanostructures, two-dimensional (2D) materials have larger specific surface area leading to greater sensitivity for target molecules, and better scalability which facilitates large-scale fabrication; thus these advantages and superior performances call for the constructions of highly effective and efficient FET biosensors [15–17]. Nevertheless, due to the absence of band gap structure, the use of graphene and its derivatives as conductive materials in FET biosensors, results in a low switch of FET, which limits the detection sensitivity of the sensor [18–20]. Molybdenum disulfide (MoS_2), on the other hand, a typical semiconducting layered transition-metal dichalcogenide (TMD), has attracted increasing attention on the basis of its tunable band gap structure compared with graphene [21,22]. It has a layer-dependent electronic band structure with excellent electrical, physical, optical and catalytic properties, which are desirable in developing new generations of electronics and optoelectronic devices [23–25]. Meanwhile, MoS_2 shows high stability in air due to a lack of dangling bonds, which significantly improves the performance of FETs for biosensing [26]. Recent reports have demonstrated MoS_2 FETs were used for electrical detection of various biomolecules. Park *et al.* [27] investigated the FET device using multi-layered MoS_2 with alumina (Al_2O_3) as a protective layer for detecting prostate specific antigen (PSA) to achieve high sensitivity, with a limit of 100 fg mL^{-1}. Lee *et al.* [28] developed MoS_2 FET devices without oxide layer for PSA detection with high selectivity, and the minimum detectable concentration was 1 pg mL^{-1}. Liu *et al.* [29] demonstrated highly sensitive FET biosensors for detection of DNA based on chemical vapor deposition (CVD)-grown monolayer MoS_2 films. It is still underdeveloped, however, in achieving effective detections in plasma and obtaining simple and highly sensitive MoS_2 FET biosensors for practical clinical applications. Herein, we demonstrate a few layered MoS_2 FET biosensors that can electrically detect FGF21 with high sensitivity and high selectivity in dry environment, without relying on an additional oxide layer on top of the conductors. MoS_2 can be directly functionalized owing to its stability and hydrophobic surface properties to simplify the immobilization process. In addition, the non-aqueous environment offering excellent reliability and repeatability was used to quickly and accurately detect FGF21, reducing the influence of leakage. The proposed MoS_2 FETs show high electrical response (i.e., a current decrease when FGF21 concentration increases), with detected FGF21 as low as 10 fg mL^{-1}. Moreover, the biosensor exhibits good selectivity for complex proteins in serum. This method can be generalized to other TMD materials, which provides a lab-on-chip platform for the preparation of biosensors and potential applications in early clinical diagnosis and biomedical research.

EXPERIMENTAL SECTION

Materials

MoS_2 was purchased from Sigma-Aldrich (USA). Silicon (SiO_2/Si) was purchased from Suzhou Research Semiconductor Co., Ltd (China). Indium (In) and gold (Au) were purchased from ZhongNuo Advanced Material (Beijing) Technology Co., Ltd (China). FGF21 antibody (Anti-FGF21) and FGF21 were purchased from R&D Systems (USA). 1-Pyrenebutanoic acid succinimidyl ester (PASE), *N*,*N*-dimethylformamide (DMF), phosphate buffered saline (PBS), bovine serum albumin (BSA) were obtained from Beijing J&K Scientific Ltd (China). Interleukin-6 (IL-6), C-reactive protein (CRP) and myoglobin (MB) were purchased from Biovision (USA).

MoS_2 FET fabrication

Thin layers of MoS_2 nanosheets were mechanically exfoliated from natural bulk materials using scotch tape and transferred on highly p-doped Si substrate with 300 nm SiO_2. The thickness of the multilayer MoS_2 flakes was determined by optical and atomic force microscopy (AFM). MoS_2 flakes with thickness in the range of 5–15 nm were used to fabricate the field-effect transistors. The channel length of our device was 10 μm according to the size of TEM-grid used as the mask, and then In/Au (5 nm/50 nm) electrodes were deposited as the source and drain electrodes (S/D) on MoS_2 by thermal evaporation, respectively. We used back gate FET to detect the bio-interaction in dry states, and the voltage was added through the back Si. To reduce the contact resistance, MoS_2 FETs were annealed at 200°C for 1 h with 100 sccm of Ar and 10 sccm of H_2 under atmospheric pressure.

Surface functionalization and biosensing process

The devices were incubated for 2 h with 5 mmol L^{-1}

PASE solution, which was composed of DMF dissolved at room temperature, washed with deionized (DI) water and blow-dried with nitrogen (N_2). Anti-FGF21 was dissolved in PBS (1×, 0.01 mol L^{-1}) solution (pH 7.2–7.4) at a concentration of 50 μg mL^{-1}. The device was placed in a 4°C refrigerator overnight in order to immobilize the anti-FGF21 and then rinsed with DI water. BSA (50 μg mL^{-1}) was used for 1 h as a blocking agent to reduce the non-specific adsorption. After being rinsed, the device was incubated at room temperature for 30 min with different concentrations of FGF21 solution from 10 fg mL^{-1} to 1 ng mL^{-1}, rinsed with DI water and dried with N_2. Serum samples were 10-fold-diluted directly without additional treatment. The concentration of FGF21 in human serum samples was increased from 10 fg mL^{-1} to 1 ng mL^{-1}. The FET was measured in dry state.

Device measurement and characterization

The optical image was obtained by Nikon H600L microscopy. The electrical transport and sensing behavior were measured with a probe station (Cascade Microtech, MPS 150) connected with Keithley Sourcemeter 2634B at room temperature under ambient conditions. AFM characterization was conducted using Bruker Dimension Icon.

RESULTS AND DISCUSSION

Working principle and characterization of MoS_2 nanosheets

Fig. 1a shows the schematic of the MoS_2 FET surface functionalization that immobilized anti-FGF21 and its interaction with FGF21. The FET channel surface was directly functionalized with PASE by van der Waals interaction between the MoS_2 surface and the pyrene group [30]. Then, anti-FGF21 was tightly immobilized onto the terminal amino group of PASE *via* a covalent bond. Finally, BSA was introduced as a blocking agent to prevent non-specific adsorption of antibody. We chose PASE as a linker molecule to directly modify the surface of pristine MoS_2, which simplified the procedure, and more importantly, strongly immobilized the biomolecules *via* van der Waals force, improving the electronic transmission performance and achieving higher selectivity than physical adsorption [31].

The typical structure of the FET biosensor with a multilayer MoS_2 as semiconducting channel is illustrated in Fig. 1b. Briefly, pristine MoS_2 FETs were fabricated by mechanical exfoliation from natural bulk materials. Optical microscopy and AFM enable us to feasibly identify the number of layers [32]. In order to improve the reproducibility of the MoS_2 FET, and achieve higher sensitivity without being affected by other interference factors, the MoS_2 with thickness in the range of 5–15 nm was selected to construct the devices. Meanwhile, contact resistance arising from the metal-semiconductor plays a key role in affecting the transistor performance [10]. Gold (Au), and indium (In) have been proved to make high-quality ohmic contact for fabricating high-performance MoS_2 transistors. Firstly, the work function of In (about 4.12 eV) is smaller than that of the n-type MoS_2 (in the range of 4.6–4.9 eV) [33]. Thus, the electron carrier ac-

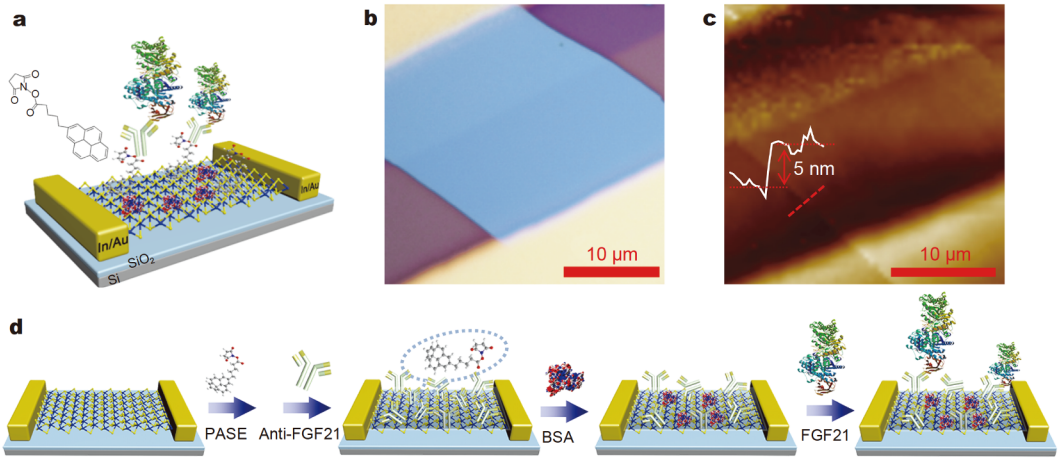

Figure 1 (a) Schematic representation of the label-free MoS_2 FET as biosensor to electrically detect FGF21. (b) Optical and (c) AFM images of the MoS_2 FET transistor. Inset in (c) shows the MoS_2 thickness. (d) Experimental process of a surface chemistry to prepare anti-FGF21 on MoS_2 surface and its reaction with FGF21.

cumulates at the In-MoS_2 interface, and no barrier exists for the electron carrier. Secondly, In and MoS_2 can form van der Waals interaction to demonstrate a low contact resistance and provide good contact, as reported in a recent study [34]. Here, 5 nm In followed by 50 nm Au were deposited as the source and drain electrodes, which can maintain the higher mobility for biosensor and also increase the adhesion force compared with gold electrodes. To demonstrate the stability of In in 1×PBS solution, we measured the electrical properties before and after treatment of the device in 1×PBS as control, and the device showed negligible current change in transfer characteristics, as shown in Fig. S1.

The electrical properties of MoS_2 FETs were characterized by measuring the transfer curve (i.e., drain-source current *versus* gate voltage, I_D–V_{GS}) and the output curve (i.e., drain-source current *versus* drain voltage, I_D–V_{DS}). Fig. S2a shows the output characteristics in which I_D increases linearly with V_{DS} within −60–60 V range of V_{GS}. The result indicates a good ohmic contact between the electrodes and MoS_2 layers. Fig. S2b exhibits the transfer curve of the same MoS_2 FET measured as the gate voltage (V_{GS}) varied from −60 to 60 V at drain voltage (V_{DS}) of 1 V, clearly indicating that the MoS_2 FET device exhibits n-type behavior. The mobility of the transistor was determined from the slope of the transfer characteristic curve (i.e., to be ~31.05 $cm^2 V^{-1} s^{-1}$) using the standard equation $\mu=(dI_D/dV_{GS})\times[L/(WC_iV_{DS})$, in which $C_i=\varepsilon_0\varepsilon_r/d_{ox}$ based on the parallel capacitor model. Our FETs made from 5–15 nm MoS_2 show typical mobilities in the range of 10–40 $cm^2 V^{-1} s^{-1}$ under the same conditions [35].

To demonstrate the immobilization of anti-FGF21 and its specific reactivity with FGF21 on MoS_2 FETs through the PASE treatment, AFM was used to characterize the surface morphology. Fig. 2a shows that the root-mean-square (R_q) roughness of the pristine MoS_2 is 0.386 nm prior to treatment. AFM images of the modified MoS_2, i) after immobilized with anti-FGF21 and ii) after its complexation with FGF21 are shown in Fig. 2b, c, respectively. Compared with the anti-FGF21 functionalization (R_q = 0.770 nm), Fig. 2c exhibits an increased value to 1.15 nm, suggesting that anti-FGF21 structure specifically bound with FGF21 after the treatment.

Electrical properties of MoS_2 FET device

In order to further verify the immobilization of antibodies, electrical responses were characterized. As shown in Fig. 3a, the current increases after the immobilization of anti-FGF21. Considering the correlation between the binding molecule and the charge distribution on MoS_2 channel, it is well-known based on the 'pH memory theory' that when the protein is dried, its ionization state in aqueous solution (1×PBS) pH is retained, and thus the chargeability remains unchanged [36,37]. Therefore, the current increase indicated that the antibody was a positive charged molecule without necessarily knowing the isoelectric point (pI) of the anti-FGF21. In order to verify the chargeability of the antibody, we directly immobilized BSA and FGF21 through the PASE molecule on the surface of pristine MoS_2, which was consistent with the conditions for immobilized anti-FGF21. As shown in Fig. 3b and c, both of the currents reduced after fixing FGF21 and BSA. The pIs of FGF21 and BSA are about 5.43 and 4.7, respectively. According to the 'pH memory theory', the pH of PBS ranging from 7.2 to 7.4 was higher than the pIs of the two proteins, leading to the negative potential of FGF21 and BSA. The negatively charged BSA and FGF21 were immobilized on the n-type MoS_2 channel, which reduced the effective gate field under positive gate bias conditions, thereby reducing the density of accumulated electrons to reduce I_D. Hence, it was demonstrated that anti-FGF21 was a positive charged molecule. After knowing the chargeability of anti-FGF21,

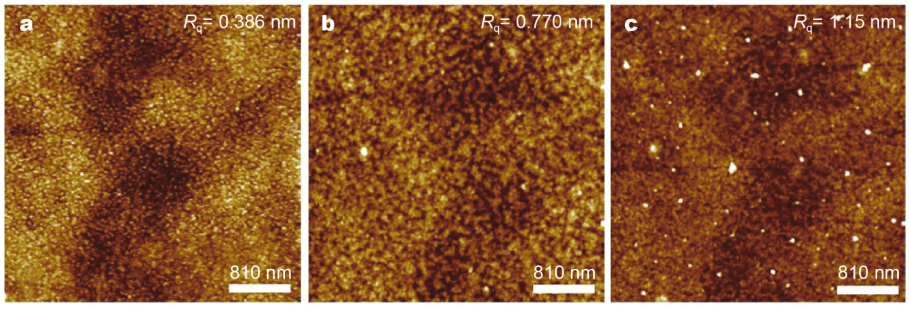

Figure 2 AFM-measured surface roughness of the same device with (a) pristine MoS_2, (b) after immobilized with anti-FGF21 and (c) after treatment with FGF21.

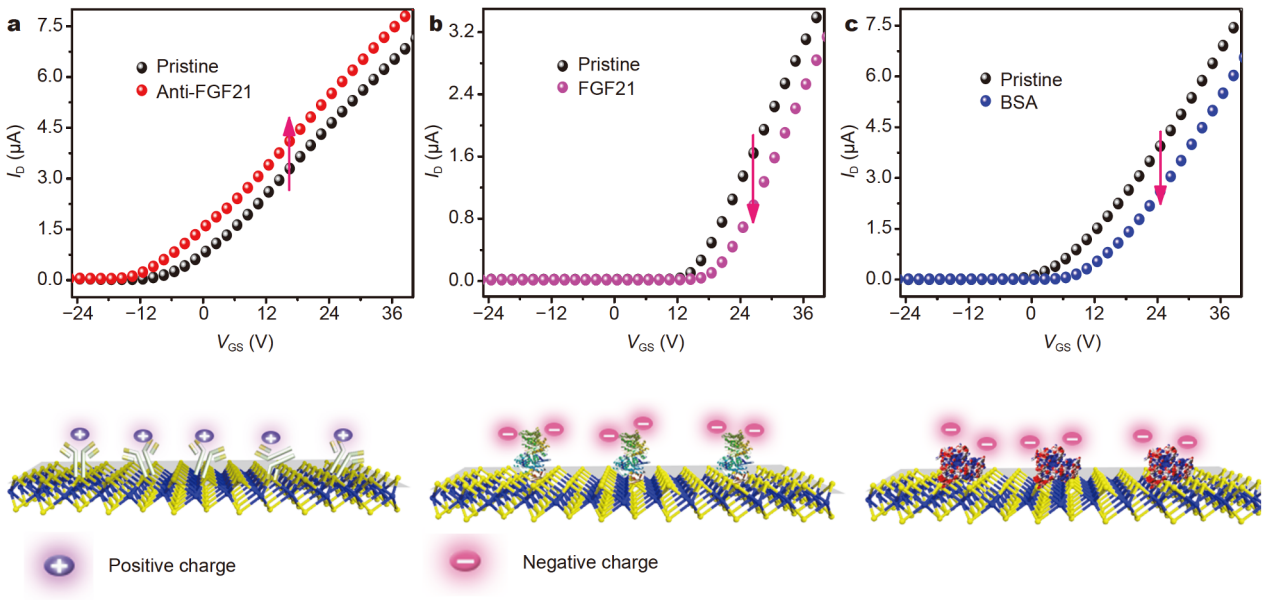

Figure 3 Shifts in the transfer curves for charge variation of immobilized targets. (a) 50 μg mL^{-1} of Anti-FGF21, (b) 1 ng mL^{-1} of FGF21 and (c) 50 μg mL^{-1} of BSA.

BSA and FGF21, we took a step-by-step observation of their current responses on another device. Fig. S3 shows the anti-FGF21 fixation led to an increase in current, consistent with the result in Fig. 3a. After BSA immobilization, the current decrease was negligible, the results indicated that most binding sites were already occupied by FGF21 antibody and just a small fraction of sites were available on the MoS_2 surface. The inevitable interference as a blocker can be ignored although BSA is negatively charged. After FGF21 was specifically combined with ant-FGF21, the current further decreased. This process can provide experimental evidence for the consecutive trends of current change caused by the FGF21 concentration gradients. The 'pH memory theory' can be utilized as an excellent theoretical basis for achieving highly accurate and reproducible biosensor operation [27].

After investigating the sensing behavior of MoS_2 transistor, the sensing mechanism behind the change of the current is further discussed. For example, a change of doping effect (charge transfer) can result in a shift of the threshold voltage (V_{th}) in transfer characteristic and change the current at any gate voltage, and changes in carrier mobility will lead to corresponding changes in the slope of the transfer characteristic transconductance [38,39]. In Fig. S3, after positively charged anti-FGF21 molecules were adsorbed, the threshold voltage in the transfer curve changed from 24.6 to 13.45 V, resulting in a negative shift, which indicated an obvious n-doping effect [40]. This effect implies that electrons in the molecule are transferred to MoS_2. The negatively charged FGF21 specifically bound to partial antibody and V_{th} changed from 13.45 to 20.79 V. Since it reduces the effect of antibodies on the surface conductivity of the MoS_2, it is equivalent to the effect of p-doping. Thereby, the amount of electron transfer in the molecule to MoS_2 is reduced, resulting in a V_{th} shifting in the positive direction relative to the antibody, while incomplete capture of the antibody results in its V_{th} being shifted to a negative direction relative to the original current. The variation of the V_{th} in different doping processes is consistent with the 'pH memory theory'.

Sensitivity of FET biosensor

Electrical measurements of anti-FGF21 binding with target FGF21 were performed on the MoS_2 channel based FETs. Fig. S4 shows that FGF21 incubation reaches equilibrium after 30 min, therefore, a 30-min incubation time was adopted for all the consecutive treatment. Under the same reaction conditions, Fig. 4a shows the transfer characteristics of the same MoS_2 FET device measured at incremental concentrations of FGF21: 10 fg mL^{-1}, 100 fg mL^{-1}, 1 pg mL^{-1}, 10 pg mL^{-1}, 100 pg mL^{-1} and 1 ng mL^{-1}. According to 'pH memory theory', anti-FGF21 retains its original chargeability during FGF21 repeated incubations. The current decreases gradually with

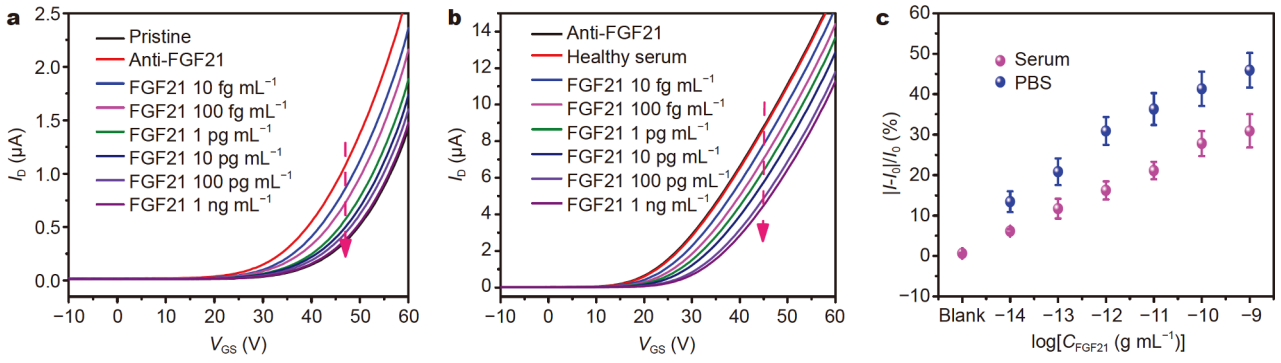

Figure 4 Transfer characteristics of functionalized MoS_2 FETs treated with different concentrations of target FGF21 ranging from 10 fg mL^{-1} to 1 ng mL^{-1} measured in (a) PBS (pH 7.2–7.4) at V_{DS} = 1 V, and (b) 10-fold diluted human serum at V_{DS} = 1 V. (c) The fractional change of the I_D for the sensing performance of the MoS_2 FET at V_{GS} = 60 V for their corresponding calibration curve in serum (purple line) and comparison for the same concentrations as measured in PBS (blue line).

increasing FGF21 concentration in the I_D–V_{GS} transfer curves, and it can be clearly seen that the current greatly varies at the concentration of 10 fg mL^{-1}. Sensitivity was determined by the absolute value of the fractional change of the I_D at V_{GS} = 60 V, against the logarithmic change of the concentrations (Fig. 4c). The fractional change in current clearly indicates a quantitative relationship in which the current decreases as the concentration of FGF21 increases from 10 fg mL^{-1} to 1 ng mL^{-1}. Meanwhile, Fig. S5 shows the V_{th} shift at different concentrations of FGF21. The V_{th} change enhanced stepwise with FGF21 concentration increasing, which indicated that the doping effect also increased. Normally, the level of FGF21 in healthy human is in range of 45.3 to 66.7 pg mL^{-1} [8,41]. This biological range is well within our device testing range. Therefore, the MoS_2 FETs demonstrated here exhibit high sensitivity and response at a low concentration of 10 fg mL^{-1} with a standard error under 3%, which also lay the foundation for rapid detection reactions and biosensing. As shown in Fig. S6, an additional parallel experiment using four sets of FGF21 concentration gradients produced similar results as those in Fig. 4, i.e., large responses for FGF21 concentrations as low as 10 fg mL^{-1} and having the same trend of current change. For FET-based biosensors, device-to-device diversity is the main challenge for their practical applications. The change in each step and batch will affect the response of the device detection, such as the thickness, the defect of the materials, the details of the fabrication, the contact between metal and semiconductors and the detection measurement condition. For MoS_2 FET biosensor, functionalization of MoS_2 is also an important process for the interactions between these 2D materials and biomolecules. In a nonaqueous environment of our experiment, there is less interference of Debye length [27]. The consistent current change result indicates that the MoS_2 FET devices we prepared have satisfactory reproducibility. The results are in good agreement with recent report. The high sensitivity and detection capability are achieved through a unique way of immobilizing anti-FGF21 on MoS_2 *via* surface functionalization. Unlike the currently reported methods for detecting FGF21 with ELISA [42], we have adopted a simple and fast approach, where the chemical surface modification of the MoS_2 FETs provides a more stable fixation/binding of anti-FGF21, which improves the sensitivity from 7 pg mL^{-1} to 10 fg mL^{-1}.

Selectivity of FET biosensor

To test the selectivity of the prepared MoS_2 FET biosensor, we chose several proteins, including IL-6, CRP and MB, as potential interferences. It has been reported that NAFLD is not only an early marker of insulin resistance but also an early indication of atherosclerosis, which is positively related to inflammation. In fact, patients identified with NAFLD significantly increase their chance of getting cardiovascular diseases (CVDs). When people have inflammation, IL-6 and CRP will increase in blood, while MB is also another commonly present protein. The MoS_2 FETs with immobilized anti-FGF21 have non-specifically bound to 10 ng mL^{-1} IL-6, CRP and MB, as shown in Fig. S7, while there is no significant change in $|I–I_0|/I_0$ without FGF21 in PBS buffer compared with FGF21 (1 ng mL^{-1}) detection. Also, small differences of $|I–I_0|/I_0$ were observed in samples containing FGF21 (1 ng mL^{-1}) mixed with 10 ng mL^{-1} IL-6, CRP and MB compared with the samples only with FGF21. Thus all these control proteins can be negligible for FGF21 detection, indicating that our MoS_2 FETs exhibit extremely

high selectivity.

Serum sample analysis

To further investigate the practical application of the proposed MoS_2 FET biosensors, we added FGF21 to healthy human serum for measurement. The serum sample was diluted 10-fold, and then different concentrations of FGF21 (i.e., 10 fg mL^{-1}, 100 fg mL^{-1}, 1 pg mL^{-1}, 10 pg mL^{-1}, 100 pg mL^{-1} and 1 ng mL^{-1}) were added into the serum, and measured with 5 different devices under same conditions, 10-fold-diluted serum sample without any treatment was used as a control (Fig. 4b and Fig. S8). As shown in Fig. 4b, the biosensor still maintained a high detection capacity in serum, i.e., high current response at 10 fg mL^{-1} FGF21 concentration. The result was similar to the I_D of the biosensor obtained in 1×PBS, where I_D decreased with the increased concentration of FGF21. The corresponding relationship of the schematic of Fig. 4b details the sensing performance of the MoS_2 FET as shown in Fig. 4c (purple dots), where $|I-I_0|/I_0$ increases with the increase of logarithmic FGF21 concentration in serum. For comparison, we showed the responses of biosensor, $|I-I_0|/I_0$, for the same concentrations of FGF21 in buffer (1×PBS) (blue dots in Fig. 4c). As the FGF21 concentration increased in PBS, the $|I-I_0|/I_0$ increased as well, but more variable than that in serum. The reason is attributable to the presence of other proteins in the serum sample. However, their interferences are almost negligible, and the biosensor shows high selectivity, indicating the potential application of the MoS_2 FET biosensors in clinical trials and analyses.

CONCLUSION

In conclusion, we have developed a reproducible MoS_2 FET biosensor capable of detecting FGF21 with high sensitivity and selectivity. The proposed MoS_2 FET biosensor relies on simple surface treatment to directly bind the antibody after a modified linker. This FET biosensor showed high sensitivity with a detection limit of 10 fg mL^{-1} (with a standard error under 3%), and in this condition, obvious current change was still observed. So we supposed that the sensor could detect trace FGF21 at concentrations lower than 10 fg mL^{-1}. Furthermore, the biosensor is also capable of detecting target FGF21 in serum, and shows great selectivity with the presence of several potential interference proteins. The lowest detectable concentration in serum is 10 fg mL^{-1}, similar to the value measured in the buffer solution. This highly sensitive and selective MoS_2 FET biosensor illustrates a promising approach to detect FGF21 in real serum, offering an important mean of early diagnosis of NAFLD. It opens new doors to utilize layered 2D materials in point-of-care diagnostic devices, for both specific biological event detection and real-time measurements.

Received 17 April 2019; accepted 26 May 2019; published online 6 June 2019

1 Moon YA, Hammer RE, Horton JD. Deletion of ELOVL5 leads to fatty liver through activation of SREBP-1c in mice. J Lipid Res, 2009, 50: 412–423
2 Estes C, Razavi H, Loomba R, *et al.* Modeling the epidemic of nonalcoholic fatty liver disease demonstrates an exponential increase in burden of disease. Hepatology, 2018, 67: 123–133
3 Fernandes DM, Pantangi V, Azam M, *et al.* Pediatric nonalcoholic fatty liver disease in new york city: An autopsy study. J Pediatrics, 2018, 200: 174–180
4 Kliewer SA, Mangelsdorf DJ. Fibroblast growth factor 21: From pharmacology to physiology. Am J Clinical Nutrition, 2010, 91: 254S–257S
5 Cuevas-Ramos D, Almeda-Valdes P, Aguilar-Salinas C, *et al.* The role of fibroblast growth factor 21 (FGF21) on energy balance, glucose and lipid metabolism. Curr Diabet Rev, 2009, 5: 216–220
6 Yilmaz Y, Eren F, Yonal O, *et al.* Increased serum FGF21 levels in patients with nonalcoholic fatty liver disease. Eur J Clin Invest, 2010, 40: 887–892
7 Li H, Fang Q, Gao F, *et al.* Fibroblast growth factor 21 levels are increased in nonalcoholic fatty liver disease patients and are correlated with hepatic triglyceride. J Hepatology, 2010, 53: 934–940
8 Zhang X, Yeung DCY, Karpisek M, *et al.* Serum FGF21 levels are increased in obesity and are independently associated with the metabolic syndrome in humans. Diabetes, 2008, 57: 1246–1253
9 Bergveld P. Development of an ion-sensitive solid-state device for neurophysiological measurements. IEEE Trans Biomed Eng, 1970, BME-17: 70–71
10 Mao S, Chang J, Pu H, *et al.* Two-dimensional nanomaterial-based field-effect transistors for chemical and biological sensing. Chem Soc Rev, 2017, 46: 6872–6904
11 Cui Y, Wei Q, Park H, *et al.* Nanowire nanosensors for highly sensitive and selective detection of biological and chemical species. Science, 2001, 293: 1289–1292
12 Patolsky F, Zheng G, Lieber CM. Nanowire-based biosensors. Anal Chem, 2006, 78: 4260–4269
13 Han ZJ, Mehdipour H, Li X, *et al.* SWCNT networks on nanoporous silica catalyst support: Morphological and connectivity control for nanoelectronic, gas-sensing, and biosensing devices. ACS Nano, 2012, 6: 5809–5819
14 Yu X, Munge B, Patel V, *et al.* Carbon nanotube amplification strategies for highly sensitive immunodetection of cancer biomarkers. J Am Chem Soc, 2006, 128: 11199–11205
15 Kalantar-zadeh K, Ou JZ, Daeneke T, *et al.* Two-dimensional transition metal dichalcogenides in biosystems. Adv Funct Mater, 2015, 25: 5086–5099
16 Xiao Y, Fu L. New designing for nanostructured 2D materials and 2D superlattices. Sci China Mater, 2018, 61: 761–762
17 Huang X, Zeng Z, Zhang H. Metal dichalcogenide nanosheets: Preparation, properties and applications. Chem Soc Rev, 2013, 42: 1934–1946
18 Liu Y, Dong X, Chen P. Biological and chemical sensors based on

graphene materials. Chem Soc Rev, 2012, 41: 2283–2307
19 Wei D, Liu Y. Controllable synthesis of graphene and its applications. Adv Mater, 2010, 22: 3225–3241
20 Wang L, Wu B, Liu H, *et al.* Low temperature growth of clean single layer hexagonal boron nitride flakes and film for graphene-based field-effect transistors. Sci China Mater, 2019, 62: 1218–1225
21 Perera MM, Lin MW, Chuang HJ, *et al.* Improved carrier mobility in few-layer MoS_2 field-effect transistors with ionic-liquid gating. ACS Nano, 2013, 7: 4449–4458
22 Kim S, Konar A, Hwang WS, *et al.* High-mobility and low-power thin-film transistors based on multilayer MoS_2 crystals. Nat Commun, 2012, 3: 1011
23 Kalantar-zadeh K, Ou JZ. Biosensors based on two-dimensional MoS_2. ACS Sens, 2016, 1: 5–16
24 Gan X, Zhao H, Quan X. Two-dimensional MoS_2: A promising building block for biosensors. Biosens Bioelectron, 2017, 89: 56–71
25 Liu S, Zhang X, Zhang J, *et al.* MoS_2 with tunable surface structure directed by thiophene adsorption toward HDS and HER. Sci China Mater, 2016, 59: 1051–1061
26 Sarkar D, Liu W, Xie X, *et al.* MoS_2 field-effect transistor for next-generation label-free biosensors. ACS Nano, 2014, 8: 3992–4003
27 Park H, Han G, Lee SW, *et al.* Label-free and recalibrated multilayer MoS_2 biosensor for point-of-care diagnostics. ACS Appl Mater Interfaces, 2017, 9: 43490–43497
28 Lee J, Dak P, Lee Y, *et al.* Two-dimensional layered MoS_2 biosensors enable highly sensitive detection of biomolecules. Sci Rep, 2015, 4: 7352
29 Liu J, Chen X, Wang Q, *et al.* Ultrasensitive monolayer MoS_2 field-effect transistor based DNA sensors for screening of down syndrome. Nano Lett, 2019, 19: 1437–1444
30 Li Z, Ye R, Feng R, *et al.* Graphene quantum dots doping of MoS_2 monolayers. Adv Mater, 2015, 27: 5235–5240
31 Huang Y, Zheng W, Qiu Y, *et al.* Effects of organic molecules with different structures and absorption bandwidth on modulating photoresponse of MoS_2 photodetector. ACS Appl Mater Interfaces, 2016, 8: 23362–23370
32 Benameur MM, Radisavljevic B, Héron JS, *et al.* Visibility of dichalcogenide nanolayers. Nanotechnology, 2011, 22: 125706
33 Gong C, Colombo L, Wallace RM, *et al.* The unusual mechanism of partial Fermi level pinning at metal-MoS_2 interfaces. Nano Lett, 2014, 14: 1714–1720
34 Wang Y, Kim JC, Wu RJ, *et al.* Van der Waals contacts between three-dimensional metals and two-dimensional semiconductors. Nature, 2019, 568: 70–74
35 Yang R, Wang Z, Feng PXL. Electrical breakdown of multilayer MoS_2 field-effect transistors with thickness-dependent mobility. Nanoscale, 2014, 6: 12383–12390
36 Costantino HR, Griebenow K, Langer R, *et al.* On the pH memory of lyophilized compounds containing protein functional groups. Biotechnol Bioeng, 1997, 53: 345–348
37 Meyers RA. Molecular Biology and Biotechnology: A Comprehensive Desk Reference. Weinheim: John Wiley & Sons, 1995
38 Zhao YL, Stoddart JF. Noncovalent functionalization of single-walled carbon nanotubes. Acc Chem Res, 2009, 42: 1161–1171
39 Heller I, Janssens AM, Männik J, *et al.* Identifying the mechanism of biosensing with carbon nanotube transistors. Nano Lett, 2008, 8: 591–595
40 Sim DM, Kim M, Yim S, *et al.* Controlled doping of vacancy-containing few-layer MoS_2 *via* highly stable thiol-based molecular chemisorption. ACS Nano, 2015, 9: 12115–12123
41 Kralisch S, Tönjes A, Krause K, *et al.* Fibroblast growth factor-21 serum concentrations are associated with metabolic and hepatic markers in humans. J Endocrinology, 2013, 216: 135–143
42 Bisgaard A, Sørensen K, Johannsen TH, *et al.* Significant gender difference in serum levels of fibroblast growth factor 21 in danish children and adolescents. Int J Pediatr Endocrinol, 2014, 2014: 7

Acknowledgements This work was financially supported by the National Natural Science Foundation of China (21705036, 21475036, 51271074, 21476066, and 81572500), the Natural Science Foundation of Hunan Province, China (2018JJ3035), Hunan Young Talents (2016RS3036) and the Fundamental Research Funds for the Central Universities from Hunan University. Prof. Guo Hong acknowledges the Start-up Research Grant (SRG2016-00092-IAPME), Multi-year Research Grant (MYRG2018-00079-IAPME) of the University of Macau, Science and Technology Development Fund (081/2017/A2, 0059/2018/A2, 009/2017/AMJ) and Macao SAR (FDCT).

Author contributions Liu S conceived the idea. Gong X and Liu Y designed the project and performed the experiments. Gong X wrote the paper with support from Liu Y. Xiang H draw the mechanism schematic. Liu H characterized the materials. Liu S and Hu T discussed the results of the experiments. All authors contributed to the general discussion.

Conflict of interest The authors declare no competing financial interest.

Supplementary information Supporting data are available in the online version of the paper.

Xinxing Gong is a postgraduate student in Professor Liu's group and will receive her master's degree from the School of Chemistry and Chemical Engineering, Hunan University in 2019. Her current research focuses on the detection of biological target molecules by 2D nanomaterial field effect transistors.

Yeru Liu got her Master degree in applied chemistry from Zhengzhou University. Now, she is a PhD student under the supervision of Prof. Song Liu at the School of Chemistry and Chemical Engineering, Hunan University. Her research interests mainly focus on the preparation of nanodevices and the application of nanomaterials in biomedicine.

Song Liu received his PhD in 2011 from Peking University. He was a postdoctoral fellow working with Prof. Liming Dai (2011–2013) in Case Western Reserve University. After 3 years' research in National University of Singapore (2013–2016), he is now a full professor in the Institute of Chemical Biology and Nanomedicine in Hunan University. His research interests focus on the controlled synthesis of low-dimensional materials, the application research of functional devices and nanobiological research.

Gang Yu received his PhD in 1999 from the Institute of Metal Corrosion and Protection, Chinese Academy of Sciences. He is now a full professor in the College of Chemistry and Chemical Engineering in Hunan University. His research interests focus on (1) synthesis, characterization and application of alloy nanowires, (2) nanostructured chemical sensors, biosensors and biomedical devices, (3) electroless plating and electrical plating on magnesium alloys and powders, and (4) transparent nanofunctional fluorocarbon coatings.

无膜且具有重现性的MoS_2场效应晶体管生物传感器用于高灵敏度和高选择性地检测FGF21

龚新星[1†], 刘业茹[1†], 向海燕[1], 刘航[1], 刘志刚[2], 赵晓蕊[1], 李继山[1], 李惠敏[1], 洪果[3], Travis Shihao Hu[4], 陈洪[5], 刘松[1*], 余刚[1*]

摘要 成纤维细胞生长因子21(FGF21)是一种用于早期检测和诊断非酒精性脂肪肝病(NAFLD)的必需生物标志物. 最近, 开发在复杂生物环境中准确有效地检测血液中低浓度FGF21的方法受到了极大的关注. 本文展示了一种无标记、简单和高灵敏度的场效应晶体管(FET)生物传感器, 用于在非水环境中检测FGF21. 通过对二硫化钼(MoS_2)表面进行功能化将抗FGF21牢固地固定在MoS_2材料上, 使该生物传感器实现检测FGF21的检测限小于10 fg mL^{-1}. 多组平行实验证明了MoS_2 FET的高度一致性和令人满意的再现性. 此外, 生物传感器对复杂血清样品中的目标FGF21具有很高的敏感度, 这表明其在NAFLD疾病诊断中具有巨大的潜在应用前景.

